SCA2003-20: AN EXPERIMENTAL AND NUMERICAL INVESTIGATION OF WATER-OIL FLOW IN VUGULAR POROUS MEDIA

F. PAIROYS, D. LASSEUX, H. BERTIN

LEPT-ENSAM, University of Bordeaux, France

This paper was prepared for presentation at the International Symposium of the Society of Core Analysts held in Pau, France, 21-24 September 2003

ABSTRACT

Vugular porous media are found in many reservoirs especially those constituted of carbonate rocks where large cavities (called vugs) resulting from complex diagenetic processes are embedded in the porous matrix. Due to their structure, these porous materials have special transport properties and optimization of oil recovery from such reservoirs requires a good description of two-phase -oil and water- flow. From a macroscopic point of view, a reliable determination of fluid flow properties such as relative permeability and capillary pressure is desirable. In this work, we present an experimental and numerical study of water-oil flow in an artificial vugular porous medium.

Model vugular samples were obtained from a sandstone core, representing the continuum and homogeneous porous matrix through which cylindrical holes, representing the vugs, were drilled. Transparent windows, placed in front of the vugs allow a direct observation of the two-phase distribution and the evolution during flow. Due to the configuration, the flow is two-dimensional and saturation maps were obtained from local saturation measurement in the porous matrix using a γ-ray attenuation technique. Drainage and imbibition cycles were performed during which direct visualization, saturation as well as pressure measurements clearly highlight the differences between the two processes in the vug and in the matrix regions. Using different density contrasts between oil and brine, the relative effect of viscous and gravity forces was investigated.

Two-dimensional numerical simulations were performed on the experimental configuration using an industrial software. The vugular core was represented by a two-region medium corresponding to the matrix and vugs respectively. Petrophysical properties of the porous matrix were assigned by fitting experimental two-phase flow results obtained on a separate but similar homogeneous core -without vugs. In the region corresponding to the vugs, a zero capillary pressure was used while different sets of oil and water relative permeabilities were tested for comparison of pressure and saturation evolution on the vugular core with experimental data.

INTRODUCTION

Vugular porous media are often encountered in carbonate formations in particular in dolomite and limestone reservoirs and are of particular importance in petroleum engineering (Archie, 1952 ; Lucia, 1999). They are typically characterized by a continuous porous matrix embedding macro-pores often referred to as cavities or vugs which characteristic length-scale is much larger - by several orders of magnitude- than the characteristic pore size of the matrix. These vugs result from the degradation of organic elements trapped in the soil or from the presence of trapped gas during rock consolidation and their size can range from millimetres to

centimetres. Depending on their distribution and size, vugs can be more or less inter-connected between them leading to different reservoir features: close to a fractured one in the case of rather continuous vug clusters, or behaving like a more complex heterogeneous structure otherwise. Their particular behaviour in the case of two-phase flow was exhibited by several authors (Ehrlich, 1971; de Zabala & Kamath, 1995; Dauba et al., 1998; Kamath et al., 2001; Moctezuma-Berthier et al., 2002) with sometimes abnormal relative permeabilities. All these results indicate that the question of two-phase flow description in this type of medium remains opened. From a more general point of view, this problem raises the question of the correct physical description of two-phase flow in a heterogeneous porous system where two regions of pure fluid zones on the one hand embedded in a region of porous matrix on the other hand can be clearly identified at the Darcy's scale. Just as for the problem of one-phase flow (Neale & Nader, 1973; Lasseux et al., 2002), two main difficulties appear. First, is the question of adequate physical models in the two regions and second is the derivation of appropriate boundary conditions at fluid/porous matrix interfaces.

Before addressing this issue, we propose in the present work a preliminary study of drainage and imbibition mechanisms in a model vugular porous medium from both experimental and numerical points of view. For the physical description, a genaralized Darcy's law approach classically used on heterogeneous porous media is considered, implying immediately the question of a correct choice of capillary pressure and relative permeabilities in the vug region. In fact, two main purposes motivated this preliminary study. First, by performing experimental oil-water displacements on model vugular cores, we aim at a phenomenological description of drainage and forced imbibition in such media by direct observation of saturation evolution in the matrix and vug regions. Second is a preliminary study on the choice of capillary pressure and relative permeability curves in the vug region if one accepts the generalized Darcy's law model as a valid one in this context. This last part of the work is addressed from a qualitative point of view.

Water-oil displacement experiments (drainage and forced imbibition) were carried out on both homogeneous and artificial model vugular cores in water wet condition, the matrix being the same for both the homogeneous and vugular cores. Vugular cores were equipped with transparent windows for direct observation of phase distribution in the vug region. Two couples of fluids were used, one for which densities are clearly different and one were densities are matched. This was motivated by the large size of the vug on the vugular cores implying a very significant effect of gravity forces which role can be highlighted by density contrast.

Since our final goal is the prediction of drainage and imbibition mechanisms on vugular media, petrophysical characteristics –capillary pressure and relative permeabilities- were first identified on the matrix by history matching 1D corresponding experimental displacements on the homogeneous cores. These data were further employed in the matrix region during numerical simulations performed on the vugular configuration. Because the vug size is much larger than the matrix pore size, a zero capillary pressure was considered in the vug region in all our simulations. Comparisons of numerical results with experimental observation made on the vugular cores are discussed considering two different sets of relative permeabilities in the vug region. Numerical simulations were performed with an industrial reservoir simulator -ATHOS- provided by IFP and Beicip-Franlab and used under laboratory conditions.

EXPERIMENTS

Drainage and imbibition experiments performed on homogeneous and vugular cores are described in this section.

Materials and method

Porous Media

We used two natural strongly water-wet Vosges sandstone (a grey one and a red one) each of them available in square cross section samples (0.05 x 0.05 x 0.4m^3). Two cores of each rock were prepared, one of 0.18m in length kept homogeneous (cores E1 and E3 for the grey and red sandstone respectively) and one of 0.21m in length used for our model vugular media (cores E2 and E4 for the grey and red sandstones respectively). Although these two rocks have different intrinsic permeabilities, their pore structures are very similar and for this reason, relative permeability and capillary pressure curves were determined from two-phase flow experiments on the red one only (core E3) and extrapolated for the grey one (core E1). Artificial model vugular cores were obtained by drilling three parallel holes of 2.5cm in diameter as represented in Figure 1. Two couples of experiments, using different fluids, were performed on heterogeneous cores.

Fluids

We used two different oils for the two couples of experiments. First a mineral refined parrafinic oil (Marcol 52 from ESSO) and, second, dibutyl-phtalate. This last fluid was chosen for its density (ρ = 1044 kg.m^{-3}) that can be matched with brine density in order to perform experiments without density contrast. This choice was motivated by the fact that, due to the size of the vugs, gravity forces might play an important role in the phase distribution inside them. Both oils were dyed to improve direct visualization of the fluids in the vugs. Water phase was a brine containing 65g/l of KI when used with dibutyl-phtalate and 40g/l of KI otherwise. Salt addition in water phase has two main purposes. First, it increases γ–ray attenuation coefficient and improves attenuation contrast with the oil phase improving accuracy of local saturation measurements and second, it allows matching water density with that of dibutyl phthalate. Physical properties of the fluids are given in Table 1.

Experimental setup

Cores were first epoxy coated. The heterogeneous ones were prepared by drilling holes as indicated above and glass windows were placed at each hole end allowing direct observation of fluids distribution inside the vugs. Each core was equipped with valves and differential pressure transducers and was connected to a pump to inject either brine or oil at constant flow-rate. Production was recorded by weighing effluents at the core outlet. Experimental data were computer recorded. A two-dimensional rig equipped with a γ-ray source and detector was used in order to measure porosity and saturation profiles. Gamma-ray attenuation technique, well known in petroleum engineering literature (Nicholls & Heaviside, 1985), is based on the comparison between an emitted γ-ray and a transmitted one through the medium. The experimental setup is represented in Figure 2.

Experimental Procedure

Experiments were performed with vug axes placed horizontally. The procedure was as follows.

1. The porous medium was air vacuumed, then fully saturated with CO_2 before injecting brine. Porosity was measured by γ-ray technique and core weighing. Both values were compared and found to be in good agreement. Brine permeability was measured at this stage.
2. Oil was injected in order to displace brine down to irreducible water saturation (S_{wi}) at a constant flow rate of 25cc/h for the brine/dibutyl-phtalate experiment ($\Delta\rho$ = 0.) and 15cc/h for the brine/Marcol experiment ($\Delta\rho$? 0.). Saturation profiles, oil recovery and

pressure drop were measured continuously. Oil relative permeability at S_{wi} is also determined at the end of the drainage process.

3. Water was injected in the core to perform imbibition at a constant flow rate of 6cc/h for the experiment with $\Delta\rho = 0.$ and 10cc/h for the experiment with $\Delta\rho \neq 0.$. Saturation profiles, oil recovery and pressure drop were measured continuously.

It is worth noting that while saturation profiles were measured by gamma-ray-technique in the porous matrix, it was directly estimated from visualization in the vugs.

This procedure was repeated on vugular cores E2 ($\Delta\rho \neq 0.$) and E4 ($\Delta\rho = 0.$) and on homogeneous core E3 ($\Delta\rho = 0.$). Porosity and intrinsic permeability only were measured on core E1 ($\Delta\rho \neq 0.$). The corresponding experimental data are given in Table 2.

Experimental Results and Discussion

Cores E1 and E3

As indicated above, drainage and imbibition were performed on core E3 only. Experimental data were fitted by history matching pressure drop and saturation fronts. To do so, we used a 1D homogeneous two-phase flow simulator in order to identify petrophysical properties of the matrix. These data are further used in two-phase flow numerical simulations on vugular cores. Water and oil effective permeabilities were identified under a classical Corey form (Corey, 1994):

$$K_o = K_o@S_{wi}\ (1-S^*)^{a_o} \quad (1)$$

$$K_w = K_w@S_{or}\ S^{*\,a_w} \quad (2)$$

while capillary pressure was identified as:

$$Pc = Pc@S_{wi}\ S^a \quad (3)$$

For core E1, $K_o@S_{wi}$ and $K_w@S_{or}$ were deduced from values on core E2 by keeping the same ratio of the corresponding quantities on cores E3 and E4. Results are gathered in table 3 and are plotted in Figures 3 and 4 for core E3.

Core E2

Drainage. Oil (Marcol 52) was injected at a constant flow rate of 15cc/h. Breakthrough was observed after 0.7 P.V. of oil injected. During the drainage process we observed that each vug is entirely oil saturated (S_o = 100%) before drainage occurs in the next one. This observation is confirmed by the pressure drop signal recorded during the drainage process represented in Figure 7. We can see three plateaus corresponding to the drainage of the vugs performing at a quasi zero capillary pressure and large values of permeabilities compared to that in the matrix. During drainage of the vugs, the front is quasi immobile in the matrix. After complete filling of the vug, the pressure signal increases corresponding to the oil penetration in the matrix where the capillary pressure is significant. Local saturation measurements in the matrix and direct visualization in the vugs show that average water saturation is equal to 0.5 in the porous matrix and almost 0. in the three vugs at the end of the drainage process, after 1.53 P.V. of oil injected.

Imbibition. Brine was injected in the core at a constant flow rate of 10cc/h. Breakthrough appeared after 0.32 P.V. of brine injected. Main results are i) imbibiton is performed simultaneously in the vugs and in the matrix and is actually faster in the matrix due to capillary effects leading to an early breakthrough; ii) at the end of the imbibition, the three vugs are completely water saturated (S_{or} = 0. in the vugs) ; iii) complete oil displacement from the porous matrix is a very slow process ; iv) residual oil saturation, S_{or}, in the matrix was measured at the end of the process to be 0.37. The three plateaus clearly observed during

drainage process, are less visible during imbibition. Water flows continuously in the porous matrix due to capillary suction (Figure 9) and partially bypasses the vugs.
Due to gravity forces, phase separation in the vugs is clearly observed. During drainage for instance, oil droplets entering a vug coalesce and move upward spontaneously to form an oil lens that grows up at the top of water.

Core E4

Drainage. Oil (dibutyl-phtalate) was injected at a constant flow rate of 25cc/h. We observed that breakthrough appeared after 0.82 P.V. of oil injected. At the end of the drainage process the three vugs are almost completely oil saturated. Due to absence of density contrast, small oil droplets appear at several locations at the vug/matrix interface. We also observed that drainage starts in a vug before the previous one is completely oil saturated. This means that the oil front is still moving in the matrix while vugs are filling up and this can possibly be explained by the fact that wettability of the rock to water is weaker with dibutyl-phtalate. The pressure drop recorded during drainage (Figure 13) shows three plateaus corresponding to the vugs filling. These plateaus correspond to a two-phase displacement in a zero capillary pressure region. However, as indicated above, pressure signal shows also that oil is flowing in the matrix while vugs are still filling up. At the end of drainage, saturation measurements indicate that S_{wi} is equal to 0.3 in the porous matrix and almost 0. in the three vugs.

Imbibition. Brine was injected in the core at a constant flow rate of 6cc/h. Breakthrough appeared after 0.28 P.V. of brine injected. This behaviour is different from that observed on the homogeneous core showing the influence of vugs on the imbibition mechanism. Oil displacement from the vugs is a very slow process that is partially completed after 4 P.V. of brine injected. However, pressure drop (Figure 15) indicates that oil is displaced from the vugs at constant pressure (zero capillary pressure). Final value of water saturation is equal to 0.56 in the porous matrix and 1 in the vugs.
Due to the absence of gravity forces, phase segregation does not really occur. During imbibition for instance, water droplets entering a vug coalesce but remains in the bulk oil.

NUMERICAL SIMULATIONS

A black oil simulator, ATHOS®, provided by IFP and Beicip-Franlab, was used for two-dimensional numerical simulations. This model has a laboratory option allowing boundary conditions that correspond to our experiments. The objective of this part is to simulate the two-phase flow displacement on our model vugular samples considered as heterogeneous porous media made of a matrix region and a vug region and to compare results in terms of pressure drop and production. Matrix relative permeability and capillary pressure are those determined from experiments on the homogeneous cores. For the vug region, a zero capillary pressure seems a reasonable choice while the choice of adequate relative permeability is partially discussed hereafter. The intrinsic permeability in this region can be estimated by a method developed elsewhere (Lasseux et al., 2002) to about $5.10^{-5} m^2$. After several tests and for numerical convenience, a permeability of 10D was chosen in this region. As a consequence, the choice of relative permeabilities seems a priori unimportant in the vugs although experimental observation shows that, for imbibition for instance, the front still moves in the matrix while two-phase flow occurs in the vugs. Although this might be explained by capillary effects, it is important to investigate the role of mobility ratios. To do so, two sets of relative permeabilities were used in the vug region. The first one, referred to as *case 1* corresponds to Corey exponents α_o and α_w equal to 0.01 and is represented in Figure 5. This ensures that mobilities are always greater in the vug region whatever the saturation. The second set, referred to as *case 2* was obtained with α_o and α_w equal to 20 and is depicted in Figure 6. For this last case, oil mobility in the vug is smaller than oil mobility in the matrix

for S* roughly greater than 0.3 while water mobility is smaller in the vug than water mobility in the matrix for S* greater than 0.7.

2D vugular model

Core E2

Drainage. Pressure drops obtained from numerical simulations during drainage in case 1 and case 2 are plotted in Figure 8. In case 1, pressure drop evolution is qualitatively in good agreement with experimental data and plateaus are correctly reproduced. Water production (i.e. volume of water produced normalized by the pore volume) at the core outlet represented in Figure 11 versus P.V. of oil injected is also in fair agreement with experimental result for case 1, although numerical simulation underestimates the production. Case 2 does not permit to correctly reproduce the overall physical mechanism as indicated by the pressure drop which is far from experimental data. Comparison of saturation evolution in the vugs also indicates that case1 seems appropriate.

Imbibition. Simulated pressure drops obtained in case 1 and 2 for imbibition process are plotted in Figure 10. From a pure comparison with experimental data (Figure 9), case 1 does not seem to be a better choice than case2. However, a comparison of saturation evolution indicates that, in case 2, vugs are completely bypassed and oil remains entrapped while the matrix is at S_{or}. This mechanism is not observed in case 1 for which saturation evolution in the vugs is in good agreement with experimental observations. A further comparison of oil production (i.e. cumulative oil volume produced normalized by the pore volume) reported in Figure 12 confirms that case 1 provides a fair description. A better agreement with the pressure drop signal could probably be achieved with a better identification of the capillary pressure in the matrix.

Core E4

Drainage. Numerical results on the pressure drop are reported in Figure 14. As for core E2, case 2 leads to a pressure drop which does not correspond to physical observations. Numerical result obtained in case 1 is in fair agreement with experimental data, although plateaus are more pronounced and final pressure drop value is overestimated. Saturation evolution is also correctly reproduced in case1 showing a sequential oil saturation of the successive vugs while in case 2, vugs remain oil saturated.

Imbibition. Pressure drop obtained in case 1 and 2 is represented in Figure 16. A clear conclusion on the choice of relative permeabilities in the vug region can not be drawn from the pressure drop comparison, although case 2 yields an excessively high final value. Comparison of experimental saturation evolution indicates that none of the two sets correctly reproduces the imbibition scenario in the vugs although case 1 seems closer to experimental observation. A better characterization of wettability of the brine/dibutyl-phtalate/rock system would be necessary to improve the capillary pressure input.

Simulations were also performed with cross shaped relative permealibities in the vug region. Results were very similar to those obtained in case 1.

CONCLUSION

In this work, we started investigating two-phase flow in model vugular porous media. Drainage and imbibition experiments were performed with and without gravity effects on artificial vugular cores which matrices were characterized by history matching experimental data obtained on homogeneous samples. Using these characteristics, two-dimensional

numerical simulations were carried out on the heterogeneous configuration. The vugular sample was treated as a two-region heterogeneous medium and two-phase flow was simulated using the classical generalized Darcy's law approach. The vug region was considered as a zero capillary pressure zone and two sets of relative permeabilities were tested for this zone: one that keeps large values of oil and water mobilities and one allowing smaller mobilities than those in the matrix over some saturation range. From this study, the following conclusions can be drawn:

1. Experiments performed with and without density contrast exhibit very different segregation process in the vugs.
2. Experiments demonstrate very different behaviour in terms of production kinetic, saturation evolution and pressure drop signals during drainage and imbibition processes. During drainage, vugs are oil saturated sequentially and while saturating, the oil/water front remains immobile in the matrix. During imbibition, early breakthrough is observed with a long-lasting production. Water saturation of the vugs is not sequential and occurs simultaneously with the matrix imbibition. This observation motivated a preliminary study on the role of relative permeabilities in the vug region in the numerical work.
3. From this preliminary study, our conclusion on the impact of the choice of relative permeabilities in the vugs is i) for drainage at least, this choice cannot be completely arbitrary. In fact, mobilities in the vugs must be kept larger than those in the matrix. Constant relative permeabilities seem satisfactory in conjunction with a large enough intrinsic permeability; ii) for imbibition, driving capillary forces in the matrix strongly govern the overall process in particular in the vug neighbourhood. More important than the choice of relative permeabilities in the vug, is a correct capillary pressure estimation in the matrix. Additional work is required to conclude on the role of vug relative permeabilities in this case.

Although generalized Darcy's law with adequate petrophysical characteristics seems satisfactory to give a macroscopic description of drainage and imbibition processes in a model vugular medium such as the one investigated here, additional work is required to a more detailed physical study of boundary conditions at the vug/matrix (or fluid/matrix) interface during two-phase flow as well as to study the role of wettability conditions.

Acknowledgements
Authors wish to acknowledge IFP for their support.

Nomenclature

DP	differential pressure (Pa)
K	intrinsic permeability (m^2)
Kro	oil relative permeability
K_o	oil effective permeability (m^2)
$K_o@S_{wi}$	oil effective permeability at irreducible water saturation (m^2)
Krw	water relative permeability
K_w	water effective permeability (m^2)
$K_w@S_{or}$	water effective permeability at residual oil saturation (m^2)
Pc	capillary pressure (Pa)
$Pc@S_{wi}$	capillary pressure at irreducible water saturation (Pa)
P.V.	pore volume (m^3)
S_w	water saturation
S_o	oil saturation

S^*	reduced saturation ($S^* = (S_w - S_{wi})/(1 - S_{or} - S_{wi})$)
α	capillary pressure exponent
α_o	Corey exponent for the oil phase
α_w	Corey exponent for the water phase
ϕ	porosity
μ	dynamic viscosity (Pa.s)
?	density ($kg.m^{-3}$)

References

1. Archie, G. E., "Classification of Carbonate Reservoir Rocks and Petrophysical Considerations", AAPG Bulletin, 1952.
2. Dauba, C., Hamon, G., Quintard, M., and Lasseux, D., "Stochastic description of experimental 3D permeability fields in vuggy reservoir cores", SCA 9828, 1998.
3. de Zabala, E. F. and Kamath, J., "Laboratory Evaluation of Waterflood Behavior of Vugular Carbonates", SPE 30780, 1995.
4. Ehrlich, R., "Relative Permeability Characteristics of Vugular Cores, Their measurement and Significance", SPE 3553, 1971.
5. Corey, A. T. "Mechanics of Immiscible Fluids in Porous Media" Water Resources Publications, 1994.
6. Kamath, J., Nakagawa, F., Meyer, R., Kabir, S. and Hobbet, R., "Laboratory Evaluation of Waterflood Residual Oil Saturation in Four Carbonate Cores", SCA, 2001.
7. Lasseux, D., Pairoys, F. and Bertin, H., "Fluid flow in vugular porous media", Poro-Mechanics II, 481-487, edited by Auriault et al., Balkema, 2002.
8. Lucia, F.J., "Carbonate Reservoir Characterization", Berlin Heidelberg, Springer-Verlag, 1999.
9. Moctezuma-Berthier, A., Vizika, O. and Adler, P., "Water-Oil Relative Permeability in Vugular Porous Media: Experiments and Simulations", SCA, 2002.
10. Neale, G.H. and Nader, W.K., "The Permeability of a Uniformly Vuggy Porous Medium", SPE 3812, 1973.
11. Nicholls, C.P. and Heaviside, "Gamma Ray Absorption Techniques Improve Analysis of Core Displacement Tests", SPE 14421, 1985.

Tables and Figures

Case ??=0	**Brine**	**Dibutyl-phthalate**
Density (g/cc)	**1.044**	**1.044**
Viscosity (cp)	**1**	**17**
g-ray attenuation coefficient (cm^{-1})	**0.574**	**0.190**
Case ??≠0	**Brine**	**Marcol 52**
Density (g/cc)	**1.025**	**0.831**
Viscosity (cp)	**1**	**11**
g-ray attenuation coefficient (cm^{-1})	**0.425**	**0.154**

Table 1- Physical properties of the fluids.

	f	K (mD)	S_{wi} matrix	S_{wi} vugs	$K_o@S_{wi}$ (mD)	S_{or} matrix	S_{or} Vugs	$K_w(S_{or})$ (mD)
E1	**0.2**	**37**	**0.50***		**24***	**0.37***		**1.5**
E2	**0.35**	**51**	**0.50**	**0.**	**33**	**0.37**	**0.**	**2**
E3	**0.2**	**80**	**0.24**		**111**	**0.48**		**3.6**
E4	**0.35**	**120**	**0.30**	**0.**	**205**	**0.44**	**0.**	**8**

Table 2- Petrophysical data. (* data were extrapolated from cores E3 and E4).

		a_o	a_w	$K_o@S_{wi}$ (mD)	$K_w@S_{or}$ (mD)	$Pc@S_{wi}$ (Pa)	a
Matrix E2	**Drainage**	**1.3**	**2.9**	**24**	**37**	**2200**	**-1.5**
	Imbibition	**1.3**	**2.9**	**24**	**1.5**	**1175**	**-1.5**
Matrix E4	**Drainage**	**1.3**	**2.9**	**111**	**80**	**1500**	**-1.5**
	Imbibition	**1.3**	**2.9**	**111**	**3.6**	**800**	**-1.5**
Vug	**Case 1**	**0.01**	**0.01**	**10000**	**10000**	**0.**	**0.**
	Case 2	**20**	**20**	**10000**	**10000**	**0.**	**0.**

Table 3- Kr/Pc coefficients used in the matrix and vug regions for numerical simulations.

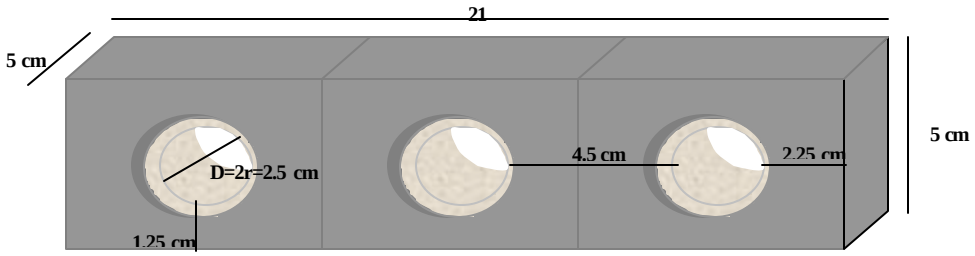

Figure 1- Geometry and dimensions of the model vugular porous media.

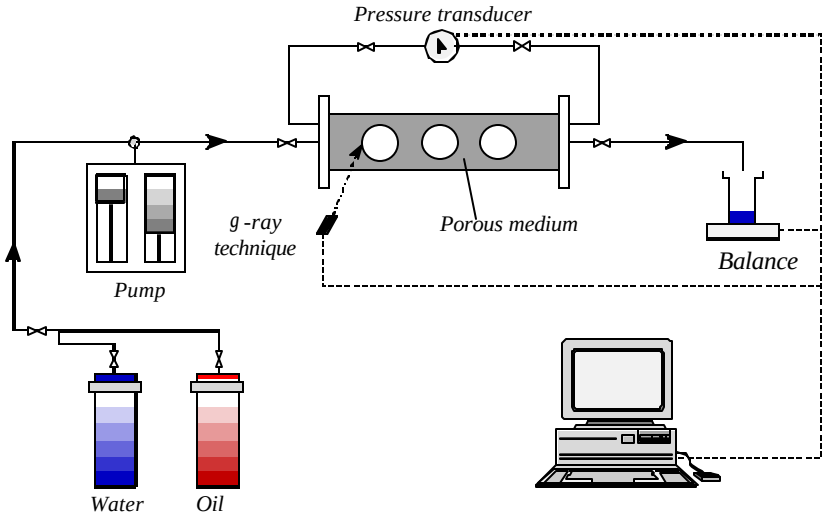

Figure 2-Experimental setup.

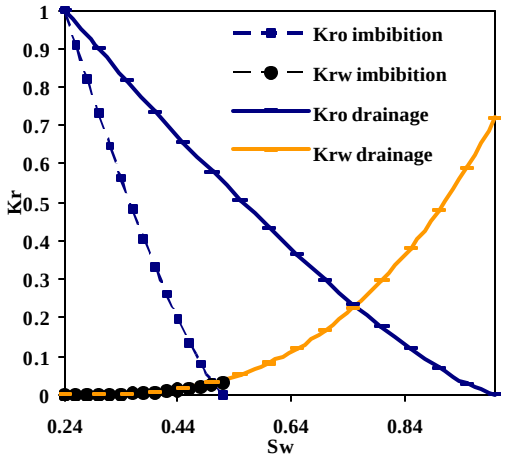

Figure 3. Kr curves identified on homogeneous core E3.

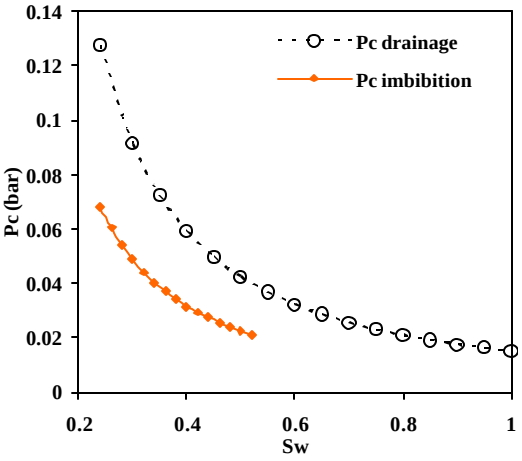

Figure 4. Pc curves identified on homogeneous core E3.

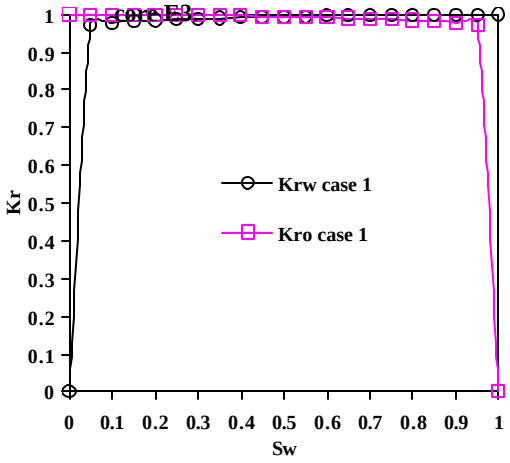

Figure 5. Kr curves in the vugs used for simulations on cores E2 and E4. Case 1

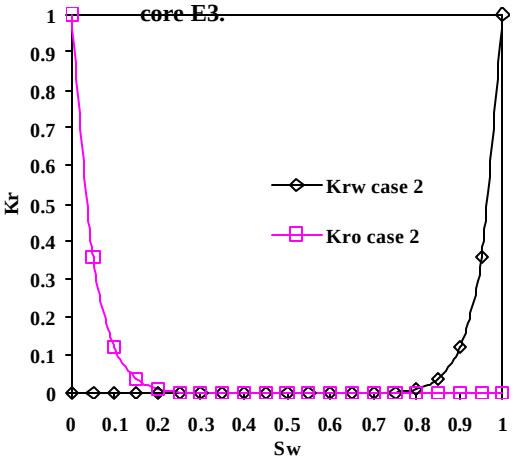

Figure 6. Kr curves in the vugs used for simulations on cores E2 and E4. Case 2

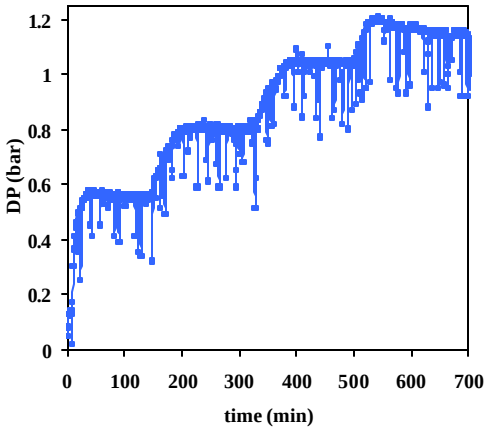

Figure 7. Experimental differential pressure obtained during drainage on core E2.

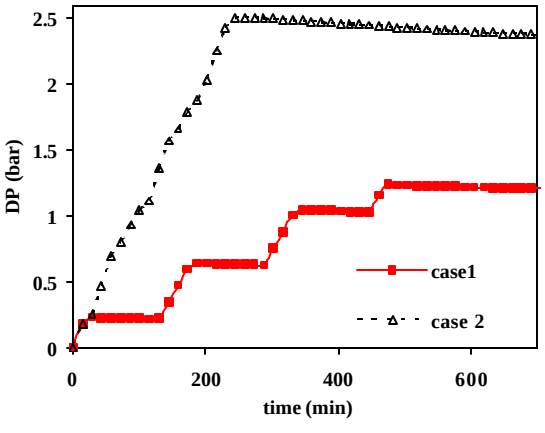

Figure 8. Numerical differential pressure during drainage on core E2. Case 1 and 2.

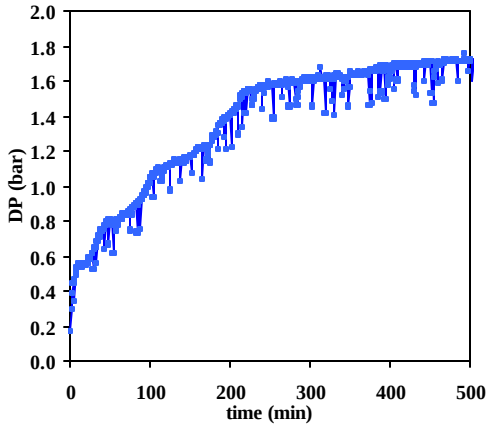

Figure 9. Experimental differential pressure during imbibition on core E2.

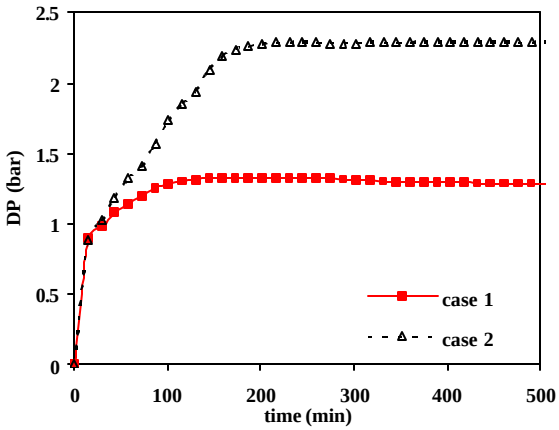

Figure 10. Numerical differential pressure during imbibition on core E2. Case 1 and 2.

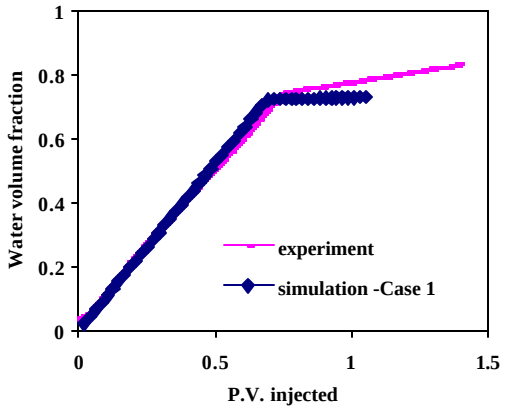

Figure 11. Water volume fraction produced versus P.V. of oil injected. Core E2.

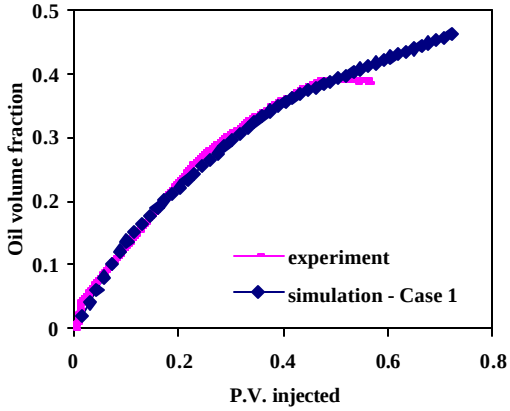

Figure 12. Oil volume fraction produced versus P.V. of water injected. Core E2.

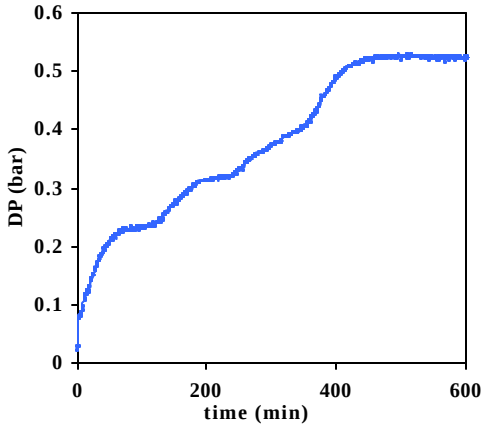

Figure 13. Experimental differential pressure during drainage on core E4.

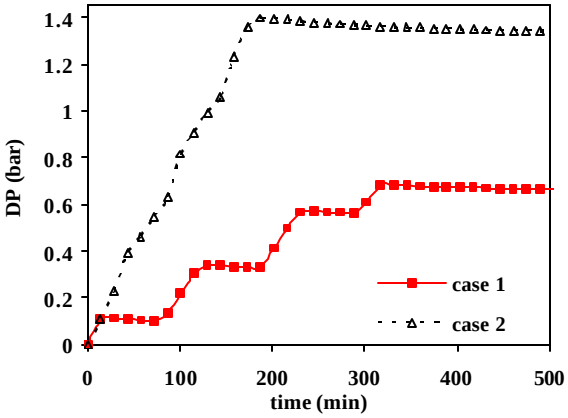

Figure 14. Numerical differential pressure during drainage on core E4. Case 1 and 2.

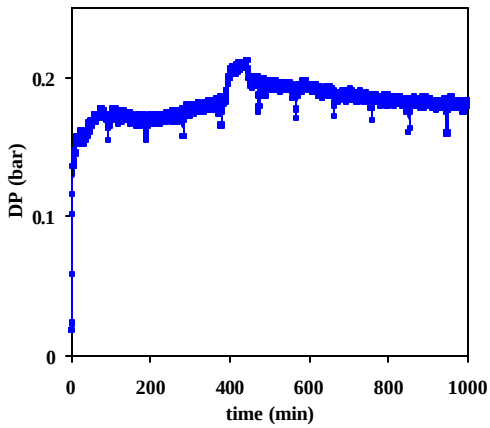

Figure 15. Experimental differential pressure during imbibition on core E4.

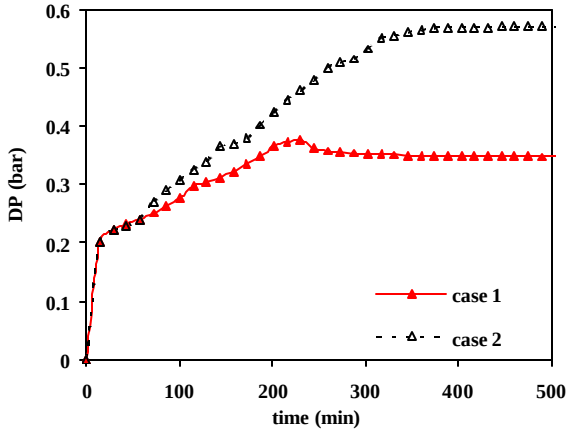

Figure 16. Numerical differential pressure during imbibition on core E4. Case 1 and 2.